

# An example of physical system with hyperbolic attractor of Smale – Williams type

S. P. Kuznetsov

November 9, 2018

*Saratov Division of Institute of Radio-Engineering and Electronics, Russian Academy of Sciences, Zelenaya 38, Saratov, 410019, Russia*

## Abstract

A simple and transparent example of a non-autonomous flow system, with hyperbolic strange attractor is suggested. The system is constructed on a basis of two coupled van der Pol oscillators, the characteristic frequencies differ twice, and the parameters controlling generation in both oscillators undergo a slow periodic counter-phase variation in time. In terms of stroboscopic Poincaré section, the respective four-dimensional mapping has a hyperbolic strange attractor of Smale – Williams type. Qualitative reasoning and quantitative data of numerical computations are presented and discussed, e.g. Lyapunov exponents and their parameter dependencies. A special test for hyperbolicity based on statistical analysis of distributions of angles between stable and unstable subspaces of a chaotic trajectory has been performed. Perspectives of further comparative studies of hyperbolic and non-hyperbolic chaotic dynamics in physical aspect are outlined.

Mathematical theory of chaotic dynamics based on rigorous axiomatic foundation exploits a notion of hyperbolicity, which implies that all relevant trajectories in phase space of a dynamical system are of saddle type, with well defined stable and unstable directions [1, 2, 3, 4]. Hyperbolic systems of dissipative type, contracting the phase space volume, manifest robust strange attractors with strong chaotic properties. The robustness (structural stability) implies insensitivity of the motions in respect to variations of equations governing the dynamics. In particular, positive Lyapunov exponent depends on parameters in smooth manner, without flops into negative region characteristic to non-hyperbolic attractors. A Cantor-like structure of the strange attractor persists without qualitative changes (bifurcations), at least while the variations are not too large. Textbook examples of these robust strange attractors are represented only by artificial mathematical constructions associated with discrete-time models, e.g. Plykin attractor and Smale – Williams attractor (solenoid).

It seems that the mathematical theory of hyperbolic chaos has been never applied conclusively to any physical object, although concepts of this theory are widely used for interpretation of chaotic behavior of realistic nonlinear systems. On the other hand, feasible nonlinear systems with complex dynamics, such as Lorenz and Rössler equations, chaotic self-oscillators, driven nonlinear oscillators etc. do not relate to the true hyperbolic class [4, 5, 6]. As a rule, observable chaos in these systems is linked with a so-called quasiattractor, a set in phase space, on which chaotic trajectories coexist with stable orbits of

high periods (usually, they are non-distinguishable in computations at reasonable accuracies). Mathematical description of quasiattractors remains a challenging problem, although in physical systems the non-hyperbolicity is masked effectively due to presence of inevitable noise. In few cases, e.g. in Lorenz model in some appropriate domain of parameter space, dynamics is proved to be quasi-hyperbolic (with some restrictions concerning violation of smoothness conditions) [7].

I am aware of only two theoretical works, which discuss examples of true hyperbolic dynamics in context of systems governed by differential equations. One relates to a system called triple linkage, which allows in a frictionless case a description in terms of orbits on a surface of negative curvature. In dissipative case, it gives rise to a hyperbolic chaotic attractor [8]. Another work deals with a 3D flow system motivated by neural dynamics and argues in favor of existence of an attractor of Plykin type in the Poincaré map associated with the flow [9].

In this Letter, I suggest an essentially simpler and transparent example of a non-autonomous flow system, which apparently manifests a hyperbolic attractor. In terms of stroboscopic Poincaré map, it is an attractor of the same kind as the Smale – Williams solenoid, but embedded in a 4D rather than 3D state space.

The system is constructed on a basis of two van der Pol oscillators with characteristic frequencies  $\omega_0$  and  $2\omega_0$ , respectively. The control parameters of the oscillators responsible for the Andronov – Hopf bifurcations in the autonomous subsystems are forced to swing slowly, periodically in time. On a half-period, the first oscillator is above the generation threshold, while the second one is below the threshold. On another half-period, a situation is opposite. Next, we assume that the first oscillator acts on the partner via a quadratic term in the equation. The generated second harmonic component serves as a primer for the second oscillator, as it comes off the under-threshold state. In turn, the second oscillator acts on the first one via a term represented by a product of the dynamical variable and an auxiliary signal of frequency  $\omega_0$ . Thus, a component with the difference frequency appears, which fits resonance range for the first oscillator and serves as a primer as it starts to generate.

Summarizing this description, we write down the following equations:

$$\begin{aligned} \ddot{x} - (A \sin 2\pi t/T - x^2)\dot{x} + \omega_0^2 x &= \varepsilon y \sin \omega_0 t, \\ \ddot{y} - (-A \sin 2\pi t/T - y^2)\dot{y} + 4\omega_0^2 y &= \varepsilon x^2, \end{aligned} \quad (1)$$

where  $x$  and  $y$  are dynamical variables of the first and the second oscillators, respectively,  $A$  is a constant designating amplitude of the slow swing of the control parameters,  $\varepsilon$  is a coupling parameter.

We assume that the period of swing  $T$  contains an integer number of periods of the auxiliary signal:  $T = 2\pi N/\omega_0$ . Thus, our set of non-autonomous equations has periodic rather than quasiperiodic coefficients. It is appropriate to treat the dynamics in terms of stroboscopic Poincaré section using a period- $T$  sequence of time instants. The Poincaré map is four-dimensional and acts in a space of vectors  $\{x, \dot{x}/\omega_0, y, \dot{y}/(2\omega_0)\}$ .

The system (1) operates as follows. Let the first oscillator have some phase  $\varphi$  on a stage of generation:  $x \propto \cos(\omega_0 t + \varphi)$ . Squared value  $x^2$  contains the second harmonic:  $\cos(2\omega_0 t + 2\varphi)$ , and its phase is  $2\varphi$ . As the half-period comes to the end, and the second oscillator becomes excited, the induced oscillations of the variable  $y$  get the same phase  $2\varphi$ . Mixture of these oscillations with the auxiliary signal transfers the doubled phase into the original frequency range. Hence, on the next stage of excitation the first oscillator accepts this phase  $2\varphi$  too. Obviously, on subsequent stages of swing the phases of the first oscillator follow approximately the mapping

$$\varphi_{n+1} = 2\varphi_n \pmod{2\pi}. \quad (2)$$

Figure 1 shows a typical pattern of time dependence of  $x$  and  $y$  from numerical solution of Eqs. (1) by Runge – Kutta method for particular parameter values  $\omega_0 = 2\pi$ ,  $T = N = 10$ ,  $A = 3$ ,  $\varepsilon = 0.5$  together with a diagram of empirical mapping for phase  $\varphi_{n+1}$  versus  $\varphi_n$ . The phases are determined at the centers of the excitation stages for the first oscillator:

$$\varphi = \begin{cases} \arctan(\omega_0^{-1}\dot{x}/x), & x > 0, \\ \arctan(\omega_0^{-1}\dot{x}/x) + \pi, & x < 0, \end{cases} \quad (3)$$

and are plotted over a sufficiently large number of the basic periods  $T$ . The mapping for the phase looks, as expected, topologically equivalent to the relation (2). (Some distortions arise due to imperfection of the above qualitative considerations and of the definition of phase; the correspondence becomes better at larger period ratios  $N$ .) Chaotic nature of the dynamics reveals itself in a random walk of humps in respect to the envelope of the generated signal on subsequent periods of swing.

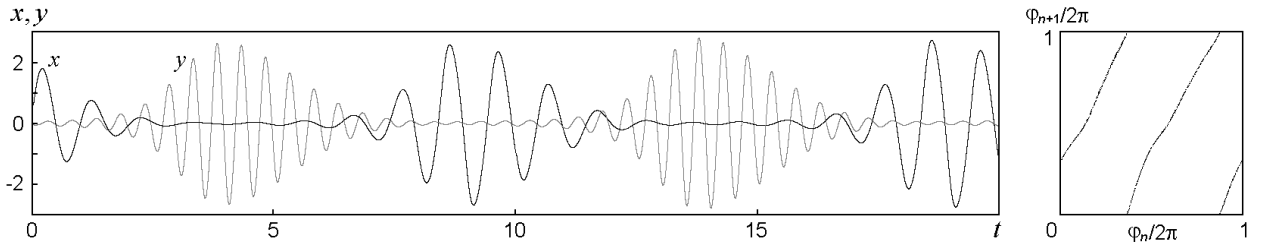


Figure 1: A typical pattern of time dependence for variables  $x$  and  $y$  obtained from numerical solution of Eqs. (1) for  $\omega_0 = 2\pi$ ,  $T = N = 10$ ,  $A = 3$ ,  $\varepsilon = 0.5$  (a) and a diagram of empirical mapping for phases of the first oscillator defined in the centers of the stages of excitation numbered by  $n$

In terms of stroboscopic Poincaré map, attractor of the system corresponds exactly to the construction of Smale and Williams. In the four-dimensional state space, the direction associated with the phase  $\varphi$  is expanding and gives rise to Lyapunov exponent estimated as  $\Lambda_1 \approx T^{-1} \log 2$ . Three rest directions are contracting, and they correspond to a three-dimensional stable manifold of the attractor. Three respective Lyapunov exponents are negative. Interpreting the stroboscopic Poincaré mapping, we may imagine a solid torus embedded in 4-dimensional space and associate one iteration of the map with longitudinal stretch of the torus, with contraction in the transversal directions, and insertion of the doubly folded “tube” into the original torus interior.

In computations, the Lyapunov exponents were evaluated with a help of Benettin’s algorithm [10, 11] from simultaneous solution of Eqs. (1) together with a collection of four exemplars of the linearized equations for perturbations:

$$\begin{aligned} \ddot{\tilde{x}} + 2x\dot{x}\tilde{x} - (A \sin 2\pi t/T - x^2)\dot{\tilde{x}} + \omega_0^2\tilde{x} &= \varepsilon\tilde{y} \sin \omega_0 t, \\ \ddot{\tilde{y}} + 2y\dot{y}\tilde{y} - (-A \sin 2\pi t/T - y^2)\dot{\tilde{y}} + 4\omega_0^2\tilde{y} &= 2\varepsilon x\tilde{x}. \end{aligned} \quad (4)$$

In a course of the solution, at each step of the integration schema, the Gram – Schmidt orthogonalization and normalization were performed for four vectors  $\{\tilde{x}(t), \dot{\tilde{x}}(t)/\omega_0, \tilde{y}(t), \dot{\tilde{y}}(t)/2\omega_0\}$ , and the mean rates of growth or decrease of the accumulated sums of logarithms of the norms

(after the orthogonalization but before the normalization) were estimated. As found, the Lyapunov exponents for the attractor at the above mentioned parameters are  $\Lambda_1 \approx 0.068 \approx T^{-1} \log 2$ ,  $\Lambda_2 \approx -0.35$ ,  $\Lambda_3 \approx -0.59$ ,  $\Lambda_4 \approx -0.81$ .

If the attractor is indeed hyperbolic, the chaotic dynamics must be robust and retain its character under (at least small) variations of the equations. As checked, this is indeed the case. In particular, the largest Lyapunov exponent is almost independent on parameters, and the rest of them manifest regular parameter dependences, as seen in Fig. 2. The left edge of the diagram corresponds to violation of the hyperbolicity.

Dynamical behavior of the same kind is observed at other integer period ratios  $N$ , including essentially smaller ones, e.g.  $N=4$ . Figure 3 shows portrait of the strange attractor in the Poincaré section in projection onto the plane  $(x, \dot{x})$  at  $\omega_0 = 2\pi$ ,  $T = N = 4$ ,  $A = 8$ ,  $\varepsilon = 0.5$ . It looks precisely as the Smale – Williams attractor should look like. Observe fractal transversal structure of “strips” constituting the attractor. For this attractor the Lyapunov exponents are  $\Lambda_1 \approx 0.167$ ,  $\Lambda_2 \approx -0.72$ ,  $\Lambda_3 \approx -1.03$ ,  $\Lambda_4 \approx -1.50$ . An estimate for fractal dimension from Kaplan – Yorke formula yields  $D \approx 1.23$ , and that from the Grassberger – Procaccia algorithm is  $D \approx 1.26$ .

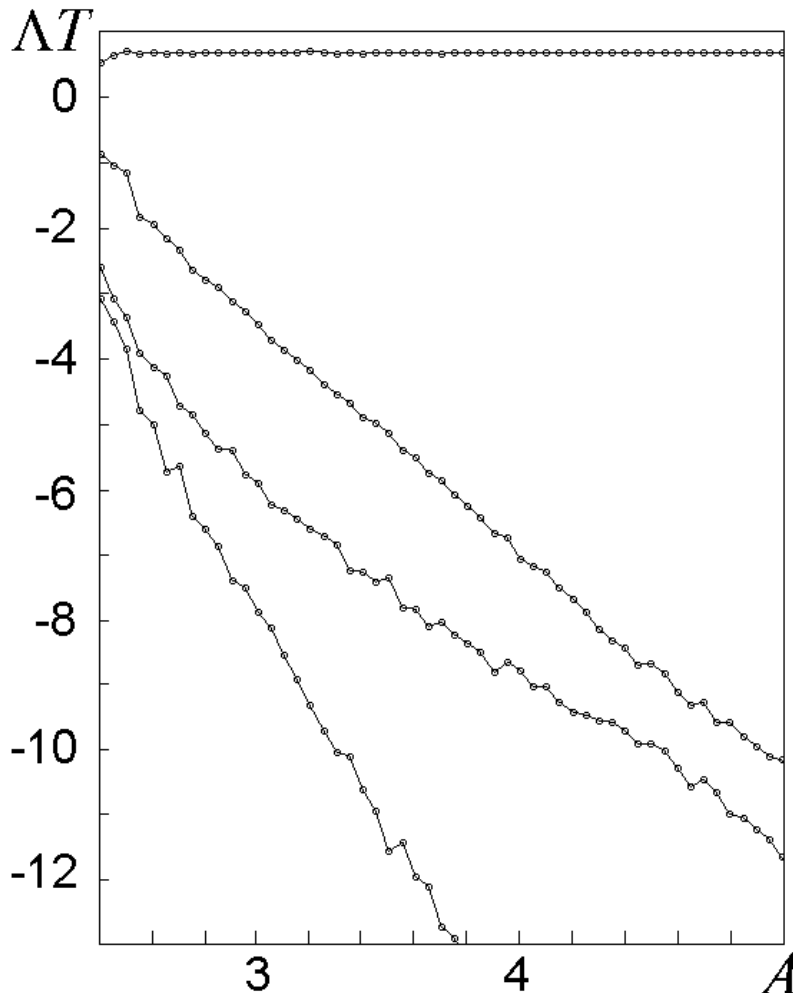


Figure 2: Computed Lyapunov exponents of the system (1) versus parameter  $A$  at  $\omega_0 = 2\pi$ ,  $N = T = 10$ ,  $\varepsilon = 0.5$ . Observe that the largest exponent remains almost constant in the whole interval of hyperbolicity being in good agreement with the estimate  $\Lambda_1 = T^{-1} \log 2$ .

It is interesting to perform a direct numerical test for hyperbolicity of the attractor. Idea of such test was suggested in Refs. [12] and [13] and applied for verification of hyperbolicity of trajectories of dynamical systems, which have one stable and one unstable directions. The procedure consists in computation of vectors of small perturbations along the trajectory in forward and inverse time with measuring angles between the forward-time and backward-time vectors at points of the trajectory. If zero values of the angle do not occur, i.e. the statistical distribution of the angles is essentially separated from zero, one concludes that the dynamics is hyperbolic. If the statistical distribution shows non-vanishing probability for zero angle, it implies non-hyperbolic behavior because of presence of the homoclinic tangencies of stable and unstable manifolds. In dissipative case these tangencies are responsible for the occurrence of quasiattractor.

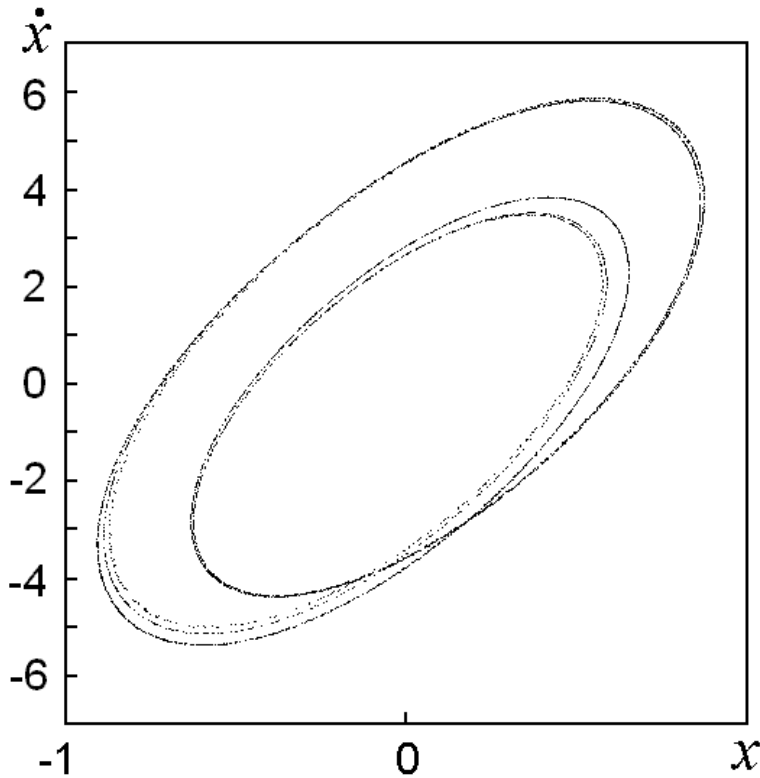


Figure 3: Portrait of the strange attractor in the stroboscopic Poincaré section  $t = 1 \pmod{N}$  in projection onto the plane  $(x, \dot{x})$  at  $\omega_0 = 2\pi$ ,  $T = N = 4$ ,  $A = 8$ ,  $\varepsilon = 0.5$

In our system (1), only unstable subspace is one-dimensional, and the stable one is three-dimensional. Therefore, the method needs a modification. An adopted algorithm consists in the following. First, we generate a sufficiently long representative orbit on the attractor  $\{x(t), \dot{x}(t)/\omega_0, y(t), \dot{y}(t)/2\omega_0\}$  from the numerical solution of Eqs. (1). Then, we solve numerically the equations (4) for a perturbation forward in time. In a course of the solution, normalization of the vector  $\mathbf{a}(t) = \{\tilde{x}(t), \dot{\tilde{x}}(t)/\omega_0, \tilde{y}(t), \dot{\tilde{y}}(t)/2\omega_0\}$  is performed after each step of integration to exclude the divergence. This vector determines an unstable direction at each point of the orbit. Next, we solve a collection of three exemplars of equations (4) in backward time along the same trajectory  $\{x(t), \dot{x}(t)/\omega_0, y(t), \dot{y}(t)/2\omega_0\}$  to get three vectors  $\{\mathbf{b}(t), \mathbf{c}(t), \mathbf{d}(t)\}$ . To avoid dominance of one eigenvector and divergence, we use the Gram – Schmidt orthogonalization and normalization of the vectors at each step of the

numerical integration. Now, at each point of the trajectory, all possible linear combinations of  $\{\mathbf{b}(t), \mathbf{c}(t), \mathbf{d}(t)\}$  define a three-dimensional stable subspace of perturbation vectors.

To estimate an angle  $\alpha$  between the one-dimensional unstable subspace and the three-dimensional stable subspace we first construct a vector  $\mathbf{v}(t)$  orthogonal to the three-dimensional subspace, with components determined from a set of linear equations  $\mathbf{v}(t) \cdot \mathbf{b}(t) = 0$ ,  $\mathbf{v}(t) \cdot \mathbf{c}(t) = 0$ ,  $\mathbf{v}(t) \cdot \mathbf{d}(t) = 0$ . Then, we compute an angle  $\beta \in [0, \pi/2]$  between the vectors  $\mathbf{v}(t)$  and  $\mathbf{a}(t)$ :  $\cos \beta = |\mathbf{v}(t) \cdot \mathbf{c}(t)|/|\mathbf{v}(t)||\mathbf{c}(t)|$  and set  $\alpha = \beta - \pi/2$ .

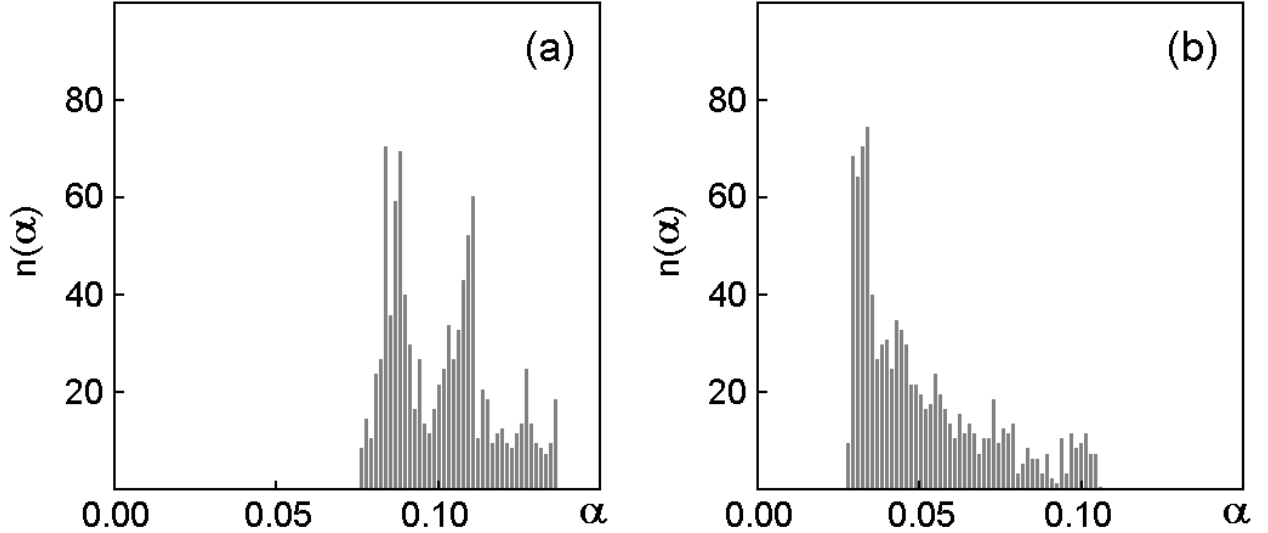


Figure 4: Histograms for distributions of angles  $\alpha$  between the stable and unstable subspaces for the system (1) with  $\omega_0 = 2\pi$ ,  $\varepsilon = 0.5$  obtained from computational procedure described in the text: (a)  $N = 10$ ,  $A = 3$  and (b)  $N = 4$ ,  $A = 8$

Figure 4 shows histogram for the distribution of angles  $\alpha$  between the stable and unstable subspaces for the system (1) obtained from computations at the two mentioned sets of parameter values. Observe clearly visible separation of the distributions from zero values of  $\alpha$ . So, the test confirms hyperbolicity of the attractors.

In spite of simplicity of the presented example, I believe it is significant as a feasible system, which may be designed as a physical device, e.g. on a basis of two interacting electronic oscillators. It opens an opportunity for experimental studies of hyperbolic chaos and its features predicted by the mathematical hyperbolic theory (robustness, continuity of the invariant measure, insensitivity of statistical characteristics of the motions in respect to noise, etc.). In addition, it makes conclusive comparative examination of dynamics of hyperbolic and non-hyperbolic systems.

In a sense, breakthrough into the hyperbolic domain is a decisive step. Now one can construct many other examples of systems with hyperbolic attractors: Because of robustness of such attractor, any variation of the right-hand parts of the equations will not destroy the hyperbolicity, at least while they are not too large. Apparently, in this way it is possible to design examples of autonomous systems with hyperbolic strange attractors as well, via modification of the system supplementing additional equations for dynamical variables, which would represent the swing and the auxiliary signals.

The author thanks A. Pikovsky and M. Rosenblum for helpful discussion. The work has been performed under partial support from RFBR (grant No 03-02-16192) and from CRDF via the Research Educational Center of Saratov University (Grant No. REC-006).

## References

- [1] A. Katok and B. Hasselblatt, *Introduction to the Modern Theory of Dynamical Systems* (Cambridge: Cambridge University Press, 1995).
- [2] V. Afraimovich and S.-B. Hsu, *Lectures on chaotic dynamical systems*, AMS/IP Studies in Advanced Mathematics, **28** (American Mathematical Society, Providence, RI; International Press, Somerville, MA, 2003).
- [3] R.L. Devaney, *An Introduction to Chaotic Dynamical Systems*, 2nd Edition (Addison-Wesley: New York, 1989).
- [4] E. Ott, *Chaos in Dynamical Systems*, 2nd Edition (Cambridge University Press, 1993).
- [5] V. S. Afraimovich and L.P. Shil'nikov, in *Nonlinear Dynamics and Turbulence*, edited by G.I. Barenblatt, G. Ioss, D.D. Joseph, 1 (Pitman, Boston, London, Melbourne, 1983); S.E. Newhouse, Publ. Math. IHES **50**, 101 (1979).
- [6] V.S. Anishchenko, V.V. Astakhov, A.B. Neiman, T.E. Vadivasova, and L. Schimansky-Geier, *Nonlinear Dynamics of Chaotic and Stochastic Systems. Tutorial and Modern Development* (Springer, Berlin, Heidelberg, 2002).
- [7] V.S. Afraimovich, V.V. Bykov and L.P. Shil'nikov, Dokl. Akad. Nauk SSSR, **234**, 336 (1977).
- [8] T.J. Hunt and R.S. MacKay, *Nonlinearity* **16**, 1499 (2003).
- [9] V. Belykh, I. Belykh and E. Mosekilde, *Int. J. of Bifurcation and Chaos* (in press).
- [10] G. Benettin, L. Galgani, A. Giorgilli and J.M. Strelcyn, *Meccanica* **15** (1980) 9.
- [11] F. Christiansen and H. H. Rugh, *Nonlinearity* **10**, 1063 (1997).
- [12] Y.-C. Lai, C. Grebogi, J.A. Yorke and I. Kan, *Nonlinearity* **6**, 779 (1993).
- [13] V.S. Anishchenko, A.S. Kopeikin, J. Kurths, T.E. Vadivasova and G.I. Strelkova, *Physics Letters*, **A270**, 301 (2000).